

Electrochemical oxidation of catecholamines and catechols at carbon nanotube electrodes

Stephen Maldonado, Stephen Morin and Keith J. Stevenson*

Received 16th May 2005, Accepted 17th June 2005

First published as an Advance Article on the web 19th July 2005

DOI: 10.1039/b506869j

The differences in the electrochemical oxidation of two commonly known catecholamines, dopamine and norepinephrine, and one catechol, dihydroxyphenylacetic acid (DOPAC), at three different types of carbon based electrodes comprising conventionally polished glassy carbon (GC), nitrogen-doped carbon nanotubes (N-CNTs), and non-doped CNTs were assessed. Raman microscopy and X-ray photoelectron spectroscopy (XPS) were employed to evaluate structural and compositional properties. Raman measurements indicate that N-CNT electrodes have *ca.* 2.4 times more edge plane sites over non-doped CNTs. XPS data show no evidence of oxygen functionalities at the surface of either CNT type. N-CNTs possess 4.0 at. % nitrogen as pyridinic, pyrrolic, and quaternary nitrogen functionalities that result in positively charged carbon surfaces in neutral and acidic solutions. The electrochemical behavior of the various carbon electrodes were investigated by cyclic voltammetry conducted in pH 5.8 acetate buffer. Semiintegral analysis of the voltammograms reveals a significant adsorptive character of dopamine and norepinephrine oxidation at N-CNT electrodes. Larger peak splittings, ΔE_p , for the cyclic voltammograms of both catecholamines and a smaller ΔE_p for the cyclic voltammogram for DOPAC at N-CNT electrodes suggest that electrostatic interactions hinder oxidation of cationic dopamine and norepinephrine, but facilitate anionic DOPAC oxidation. These observations were supported by titrimetry of solid suspensions to determine the pH of point of zero charge (pH_{pzc}) and estimate the number of basic sites for both CNT varieties. This study demonstrates that carbon purity, the presence of exposed edge plane sites, surface charge, and basicity of CNTs are important factors for influencing adsorption and enhancing the electrochemical oxidation of catecholamines and catechols.

Introduction

Graphitic carbons have been used extensively as electrode materials in biochemical electroanalysis.^{1–4} Although their malleability, chemical/electrochemical inertness, and high conductivity make graphitic carbons generally attractive for sensing applications,⁵ carbons derived from different precursors and subjected to different processing conditions exhibit varied electrochemical behaviors and sensitivities for many analytes, particularly catecholamines. Pujol and coworkers,⁶ Saraceno and Ewing,⁷ and McCreery and coworkers^{8,9} have shown that the oxidation of many catecholamines can exhibit sluggish electron transfer kinetics at “classic” carbon electrodes, *i.e.* glassy carbon (GC), basal plane highly oriented pyrolytic graphite (HOPG), and polyacrylonitrile (PAN) carbon fibers, unless rigorous steps are taken to eliminate surface contaminants and to increase exposed edge plane sites. Catecholamine oxidation and electron transfer rates may be greatly accelerated through pretreatment processes such as anodic surface activation,^{10–12} heat treatment,^{13–15} or sequestration to eliminate adsorbed impurities.¹⁶ While these processing steps lead to improved electron transfer kinetics, the reproducibility and stability of the enhanced electrochemical

performance is variable^{6,7,17} and/or short lived.^{10,18} Hence, while surface modifications/pretreatments of classic carbons have been valuable for elucidating relevant and influential surface characteristics, the inherent variability and instability of processing conditions suggest a need to design and synthesize carbon materials that already possess inherently optimized material characteristics (*i.e.* porosity, conductivity, crystallinity, surface functionalities,... *etc.*) essential for development of reliable, stable, and low cost electroanalytical applications.

Nanocarbons¹⁹ are an emerging class of graphitic carbons that can be chemically/electrochemically active as prepared.^{19–22} Carbons made *via* this route generally involve gas phase precursors rather than the liquid or solid precursors used for typical classic carbon production.¹⁹ The gas phase nanocarbon synthesis offers exceptional promise for regulated control of nanocarbon properties. For instance, the lower carbonization temperatures and pressures employed, coupled with subtle changes in temperature, pressure, carbonization catalyst, and carrier gas, can more systematically control the resultant physicochemical properties such as heteroatom doping, crystallinity, and degree of exposed edge plane sites. For biogenic amine detection, several groups have reported active nanocarbons,^{23,24} particularly nanotubes/nanofibers,^{25–28} as alternative electrode materials. Unfortunately, the specific mechanism(s) and physicochemical properties of the nanocarbons have not been well detailed.^{29–31}

Department of Chemistry and Biochemistry, Center for Nano- and Molecular Science and Technology, Texas Materials Institute, The University of Texas at Austin, Austin, Texas, 78712

Thus, desired improvements in electroanalytical figures of merit (*e.g.* sensitivity, selectivity, detection limit... *etc.*) for electrooxidation of catechols and catecholamines have not been comprehensively documented.

Previously, we have demonstrated the ability to synthesize multiwalled carbon nanotubes (CNTs) from a floating catalyst chemical vapor deposition (CVD) method that exhibited enhanced characteristics for the electroreduction of oxygen.³² Regulation of the growth conditions allowed for careful tuning of carbon structure, texture, and composition to systematically enhance the heterogeneous catalysis for hydrogen peroxide and oxygen electrocatalysis.³³ We ascribed the observed enhancements to the increased disorder and presence of surface nitrogen functionalities. In this report, we present evidence on the evaluation of electrochemical activity of “as prepared” non-doped and nitrogen-doped CNT (N-CNT) electrodes containing 4.0 at. % nitrogen for dopamine, norepinephrine, and dihydroxyphenylacetic acid (DOPAC) oxidation. As we have shown earlier for electroreduction of oxygen, our results highlight the unique character of N-doped nanocarbons towards electrooxidation of catecholamines and catechols.

Experimental

CNT electrode preparation

Ferrocene (99%, Aldrich) was used as received as the growth catalyst. Xylenes (Aldrich) and pyridine (Aldrich) were used as carbon and carbon-nitrogen sources, respectively, and were dried and distilled fresh before use. Non-doped CNT and N-CNT electrodes were prepared *via* a floating catalyst CVD process³⁴ using the same dual heated zone system and methodology as reported earlier.³³ Briefly, 1.0 ml of a 20 mg ml⁻¹ ferrocene–solvent mixture was injected at 0.1 ml min⁻¹ into the first heated zone (130–150 °C), volatilized, and carried downstream by the carrier gas (Ar–H₂ or Ar for non-doped or N-CNTs, respectively) at a total flow rate of 575 sccm. Upon reaching the second zone, the starting materials were pyrolyzed at 700 °C or 800 °C, respectively, resulting in the deposition of CNTs directly onto a nickel mesh substrate (Alfa Aesar, 100 mesh gauze, 150 µm bar width, 150 µm spacing) located in the center of the second zone, as reported previously.³³ The growth of CNTs from ferrocene–xylene or pyridine mixtures occurs *via* a base-catalyzed, diffusion-controlled mechanism where iron nanoparticles serve as nucleation sites with CNTs growing upward as reactant molecules dissociate and dissolve on the molten catalytic surface.³³ The produced material consists of carpet- or felt-like structures of carbon nanotubes that are fairly uniform and aligned normal to the nickel mesh support, with lengths greater than 10 µm and diameters ranging from 20–40 nm. After deposition, the CNT-coated nickel mesh substrates were cooled to room temperature under flowing argon (99.997%, Praxair), removed, and stored in air tight vials prior to analysis.

XPS analysis

X-Ray photoelectron spectra of CNT films were collected with a PHI 5700 ESCA system possessing an Al K-alpha

monochromatic line (1486.6 eV), calibrated with the signals for Au4f_{7/2}, Ag3d_{5/2}, and Cu2p_{3/2}. The C1s spectra were obtained in a single scan.

pH_{pzc} analysis

The pH of point of zero charge (pH_{pzc}) for undoped and N-doped CNTs were determined using mass titration analysis.³⁵ Briefly, approximately 60 mg of non-doped CNT or N-CNT was dispersed in 3 ml of 0.1 M KNO₃ (Fisher, 99.8%) made with boiled NANOpure[®] water (Barnstead, 18 MΩ cm). The ~2 wt. % suspension was capped, purged with N₂ (Praxair), and agitated for 24 hours. The pH of the slurry (no filtration) was then measured and recorded as the pH_{pzc} value. Measurements were done in triplicate.

Carbon basicity analysis

Iodometric analysis was conducted as described by Oliveira *et al.*³⁶ Dried K₂Cr₂O₇ (99.98%, Fisher), Na₂S₂O₃ (99.8%, Fisher), and starch indicator (99.6%, MCB reagents) solutions were prepared with NANOpure[®] water. I₂ (99.8%, Fisher) was dissolved with excess NaI (99.7%, Baker) to generate I₃⁻. The Na₂S₂O₃ and I₃⁻ solutions were stored in covered containers to avoid light exposure. 0.1 M Na₂S₂O₃ solutions were standardized with 0.05 M K₂Cr₂O₇ and NaI and then used to standardize the 0.05 M I₃⁻ solution. 10 ml of I₃⁻ solution and 20 mg of either non-doped CNTs or N-CNTs were collected in a clean 25 ml round bottom flask with a stir bar. The flask was then sealed with a septa, covered completely with aluminium foil, purged with nitrogen (99.999%, Praxair), and vigorously stirred for 24 hours. The CNT suspension was then filtered through a 60 ml medium porosity glass frit filter. Approximately 90 ml of NANOpure[®] water was used to rinse off I₃⁻ solution from the CNTs. The excess I₃⁻ filtrate was immediately back titrated with Na₂S₂O₃ until a golden yellow color was seen. 800 µl of starch indicator was added, resulting in a deep blue solution. Further Na₂S₂O₃ was titrated until the solution became clear, denoting the endpoint. Measurements were done in triplicate.

Raman analysis

Raman analysis on CNT films was performed with a Renishaw In Via system using 514.5 nm incident radiation. A 50 × aperture (N.A. = 0.75) was used, resulting in an approximately 2 µm diameter sampling cross section. Spectra were acquired with a single scan and a laser power density of approximately 3 mW cm⁻² and 10 s acquisition times.

Electrochemical analysis

All electrochemical studies were conducted at room temperature (23 ± 2 °C) and were performed with a CH Instruments 700A potentiostat. All aqueous solutions were made with NANOpure[®] water. A single-compartment, three electrode, glass electrochemical cell was employed for cyclic voltammetry studies. The CNT electrodes were dipped into the solution, oriented perpendicular to the cell bottom. Platinum mesh (Aldrich) and Hg/Hg₂SO₄ (sat'd K₂SO₄, CH Instruments) were used as the counter and reference electrodes, respectively.

All electrode potentials are reported *versus* Hg/Hg₂SO₄ (sat'd K₂SO₄), which is *ca.* 0.64 V positive of NHE. A commercial glassy carbon (GC) electrode (AFE2M050GC, PINE Instruments) was polished to a mirror finish with 0.3 μm and 0.05 μm alumina slurries on microcloth (Buehler), sonicated for ~30 minutes after polishing, and used immediately, as described by McCreery and coworkers.³⁷ Before each subsequent use, the GC electrode was repolished with 0.05 μm silica and sonicated for ~30 minutes.

Both the non-doped and N-doped CNT electrodes were first cycled from 0.4 V to -1.5 V at 0.1 V s⁻¹ in O₂ saturated 1 M KNO₃ (Aldrich) until they were visibly wet and a stable O₂ reduction CV was obtained. No changes in the voltammetric response were seen after extended cycling (*n* > 20). The electrodes were then removed, rinsed sequentially in three separate water volumes, immersed in deaerated 4 mM K₃Ru(NH₃)₆-1 M KNO₃, and subjected to chronocoulometric analysis for measurement of geometric electrode area.³³ Area values were used to calculate the current densities for all reported voltammograms. The electrodes were rinsed again, placed in catecholamine solutions for voltammetric analysis, and immediately analyzed by voltammetry upon immersion. For each analyte, at least three different electrodes of both CNT types were used.

Dopamine (98%, Aldrich), (-)-norepinephrine (98%, Aldrich), and dihydroxyphenylacetic acid (98%, Aldrich) were used as received. Acetate buffer from glacial acetic (99.8%, Aldrich) and potassium acetate (99.18%, Aldrich) with a resultant pH of 5.8 and ionic strength, *μ*, of 0.1 M was used as supporting electrolyte. Argon was bubbled through the test solutions for 20 minutes prior to the start of the measurements to purge the solutions of O₂. All electrochemical measurements were taken with a quiescent solution. Solution volumes were ~5–7 ml.

Convolution of obtained cyclic voltammograms was carried out through the semiintegral data processing function of the CH Instruments 700A software. Observed oxidation rate constants (*k*_{obs}^o) were estimated from peak separations in uncorrected voltammograms by the method of Nicholson.^{8,38}

Results and discussion

XPS analysis

Fig. 1 displays representative C1s spectra for non-doped CNTs and N-CNTs. The peak positions for the non-doped CNTs and N-CNTs are 284.4 eV and 284.7 eV, respectively, with full widths at half maximum (FWHM) values of 0.6 eV and 1.1 eV, respectively. The shifted peak position and larger FWHM of the N-CNTs denote a more disordered character, *i.e.*, higher edge plane content per cm²,³⁹ relative to that of non-doped CNTs. These results are consistent with previous TEM observations.³³ Observable C1s side bands suggestive of the presence of phenolic, carbonyl, and carboxylic acid oxygen functionalities have been reported for mildly and heavily oxidized carbon materials in the 286–289 eV shoulder region.^{40,41} No such signatures on the high energy side are seen for non-doped CNT and N-CNT electrodes, indicating that neither CNT variety possesses significant oxygen functionalities as prepared. The small, broad band near 291 eV

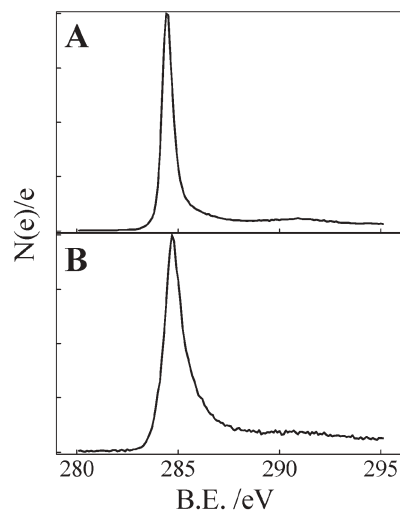


Fig. 1 Normalized X-ray photoelectron C1s spectra of (A) non-doped CNTs, and (B) N-CNTs.

visible for both CNTs is assigned to the π - π^* interband, commonly seen in graphitic carbon XPS spectra.⁴² C1s spectra obtained on electrochemically conditioned CNT electrodes did not differ significantly after use (data not shown). Neither type of CNT electrodes were subjected to anodic surface oxidation conditions^{6,14} and no voltammetric couples indicative of electroactive oxygen functionalities were observed in voltammograms of deaerated electrolyte without catecholamines. Therefore, it is unlikely that large amounts of subsequent oxygen functionalities were introduced to the surfaces of either CNT type during electrochemical study.

The total surface iron contents for the non-doped and N-CNTs were 1.2 and 1.1 at. %, respectively.³³ These earlier studies suggest that the majority of iron for both CNT types is contained within the CNT interior and encapsulated by graphene layers.³³ Additionally, previous XPS studies from our group³³ of the nitrogen doped CNT electrodes prepared under the same conditions possessing 4.0 at. % surface nitrogen indicate that nitrogen is coordinated as pyridinic-like, pyrrolic-like, and quaternary-like arrangements. The existence of nitrogen functional groups is significant enough to impart a basic nature to the N-CNTs, measuring an average pH_{pzc} value of 9.2 ± 0.4, consistent with other reports of alkaline pH_{pzc} values for nitrogenated-carbons,^{43,44} whereas the non-doped CNTs have an average pH_{pzc} value of 8.0 ± 0.4. Iodometric titrations performed on suspensions of both CNT varieties also support the increased basicity of N-doped CNTs where nitrogen-containing CNTs contained 2.3 ± 0.3 meq g⁻¹ basic sites compared to 1.5 ± 0.3 meq g⁻¹ for non-doped CNTs.

Raman analysis

Fig. 2 shows the differences in the first order Raman spectra of non-doped and N-doped CNTs. It is evident that both the D band (*circa* 1360 cm⁻¹) and G band (*circa* 1580 cm⁻¹) have larger FWHMs for N-CNTs than for non-doped CNTs and a broad shoulder below 1300 cm⁻¹ is present for N-CNTs. As described by Tascon and coworkers,⁴⁵ broader first order

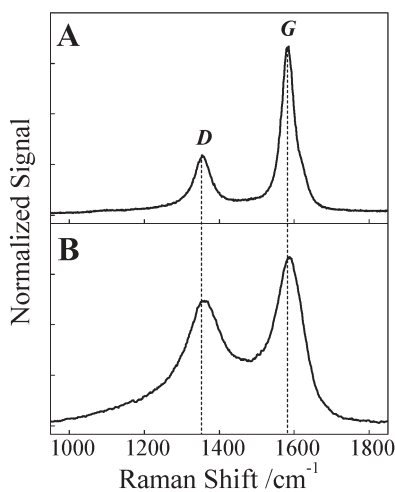


Fig. 2 First order Raman spectra for as prepared (A) non-doped CNTs, and (B) N-CNTs.

Raman bands and a shoulder on the D band qualitatively denote increased disorder in N-CNTs relative to the non-doped CNTs. Quantitative assessment of the average microcrystalline region size from the relative ratios of the D and G bands⁴⁶ as described by Tuinstra and Koenig⁴⁷ give values of 8.3 nm and 3.4 nm for the average microcrystalline region size in non-doped CNTs and N-CNTs, respectively. Hence, for a given length, N-CNTs possess roughly 2.4 times more edge plane sites than non-doped CNTs. Analysis of the low frequency Raman spectral range from 200–600 cm^{-1} yields no evidence for the presence of single walled CNTs or for iron oxide (Fe_2O_3) on the CNT surface which could result from air oxidation of Fe nanoparticles formed during the pyrolysis process.³³

Voltammetry of catecholamines

Dopamine has been used extensively as a standard redox probe to assess electrocatalysis at carbon electrodes because it undergoes inner sphere type oxidation that is very sensitive to the nature of the carbon electrode interface.^{9,10,13,16,48} Cyclic voltammograms for dopamine oxidation at non-doped CNT, N-CNT, and polished GC electrodes are shown in Fig. 3. For all three electrode types, the onset of oxidation current was ~ -0.25 V. The observance of a single set of peaks for both CNT types (Fig. 3A) is significant because it offers insight both on the spatial dispersion of active sites and on the susceptibility of those sites to surface poisoning. Only one set of peaks for both CNT types implies that facile electron transfer sites are sized and spaced far less than \sqrt{Dt} (~ 20 μm for $\nu = 0.1$ V s^{-1}) since multiple sets of peaks for the voltammetry of a given diffusional redox couple occur when the spatial separation of higher activity electron transfer sites in between much lower activity sites is large.⁴⁹ As the association between electrochemically active sites and edge plane graphite is well documented,^{13,31,50} it is not surprising that the observed current densities for N-CNT electrodes are larger than for non-doped CNTs. Indeed, this is reflective of enhanced adsorptive character for N-CNTs. While direct determination of weak adsorption in the voltammograms in Fig. 3A is difficult, deconvolution of diffusive

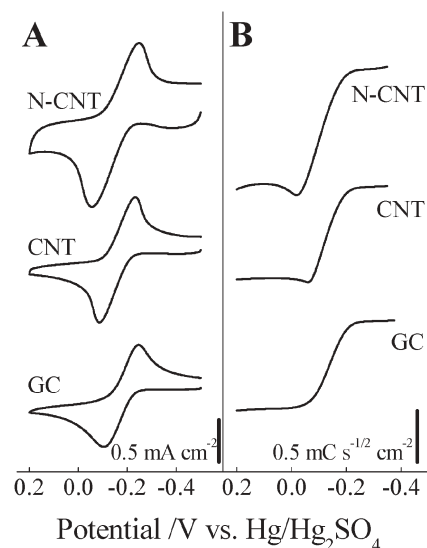


Fig. 3 (A) Cyclic voltammograms of 1.5 mM dopamine in 0.1 M acetate buffer (pH = 5.8) at N-CNT (top), non-doped CNT (middle), and GC (bottom) electrodes. Scan rate = 0.1 V s^{-1} . (B) Semiintegrals of oxidative portion of corresponding voltammograms.

and adsorptive voltammetric components is possible through semiintegral analysis,⁵¹ from which surface concentrations of adsorbed species may be estimated. The semiintegrals in Fig. 3B for both non-doped CNTs and N-CNTs show indication of weak adsorption, *i.e.*, both semiintegrals show evidence of peaks. In contrast, the sigmoidal semiintegral for GC in Fig. 3B is demonstrative of negligible dopamine adsorption.⁹ The relative differences in semiintegral peak heights for the two CNT varieties indicate that the surface coverage, Γ (mol cm^{-2}), of dopamine adsorption is at least double for the N-CNTs, which suggests that the total active surface area for dopamine oxidation of N-CNTs is larger for non-doped CNTs. We have also estimated the apparent oxidation rate constants by analysis of voltammetric peak splitting. The larger ΔE_p at N-CNT electrodes for the $2e^-$ dopamine/dopamine orthoquinone couple (*cf.* 141 mV, 145 mV, and 190 mV for GC, non-doped CNTs, and N-CNTs, respectively) suggests that the overall oxidation process is less facile at the N-CNTs (*i.e.*, k_{obs}^o is smaller by an order of magnitude). Kuwana and coworkers¹⁷ and McCreery and coworkers^{52,53} have shown that favorable dopamine oxidation is not observed at GC unless the surface is carefully cleaned of adsorbed impurities. We have also noted that unless the polishing procedure for GC electrodes is scrupulously kept clean, k_{obs}^o for dopamine oxidation can be suppressed by ~ 2 orders of magnitude, as evidenced by the 145 mV increase in peak splitting in Fig. 4 which translates to a decrease in k_{obs}^o from $\sim 10^{-3}$ to 10^{-5} cm s^{-1} . Sonication after the final GC polishing step is necessary for removal of physisorbed alumina particles and organic impurities from active sites, but short sonication times leave significant adsorbed impurities that slow dopamine oxidation. Since no cleaning or pre-treatment procedures were performed on either type of CNT electrodes, it is evident that the CNTs are both clean of adsorbed impurities and have a high density of closely-spaced available active sites for fast electron transfer “as prepared”. The cyclic voltammetry in Fig. 5 for the oxidation of norepinephrine, a catecholamine with similar

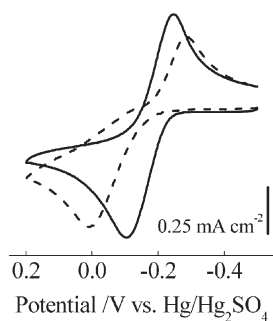


Fig. 4 Cyclic voltammograms of 1.5 mM dopamine in 0.1 M acetate buffer (pH = 5.8) at a GC electrode sonicated for 2 minutes (dotted line), and for 30 minutes (solid line) after 0.05 μm alumina polishing step. Scan rate = 0.1 V s^{-1} .

size and $\text{p}K_{\text{A}}$ to dopamine (*cf.* 8.92 and 8.88 for dopamine and norepinephrine, respectively),⁵⁴ also shows both a larger ΔE_{p} and a more peak-shaped semiintegral for N-CNTs relative to both the non-doped CNTs and GC (Fig. 5A and B). Again, the difference in ΔE_{p} values for the N-CNT and non-doped CNT norepinephrine voltammetry denotes less than an order of magnitude decrease in k_{obs}° for N-CNTs. The smaller k_{obs}° at N-CNTs for both the dopamine and norepinephrine orthoquinone couples may be rationalized considering that both dopamine and norepinephrine as well as the N-CNTs are positively charged at pH 5.8 due to their respective $\text{p}K_{\text{A}}$ and pH_{pzc} values, resulting in an unfavorable electrostatic interaction that can influence protonation and/or electron transfer steps in catecholamine oxidation. Similar arguments have been made for the observation that negatively charged carbon surfaces show improved reversibility for cationic dopamine oxidation, but poorer reversibility for DOPAC, a structurally similar yet anionic catechol.^{7,51,55} For N-CNTs, this suggests that cyclic voltammetry for negatively charged DOPAC

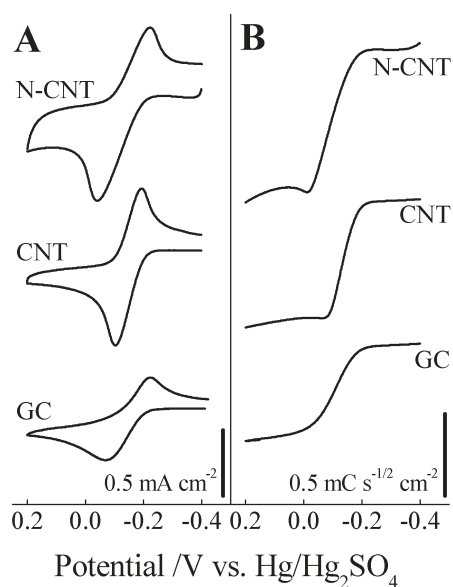


Fig. 5 (A) Cyclic voltammograms of 1.3 mM norepinephrine in 0.1 M acetate buffer (pH = 5.8) at N-CNT (top), non-doped CNT (middle), and GC (bottom) electrodes. Scan rate = 0.1 V s^{-1} . (B) Semiintegrals of oxidative portion of corresponding voltammograms.

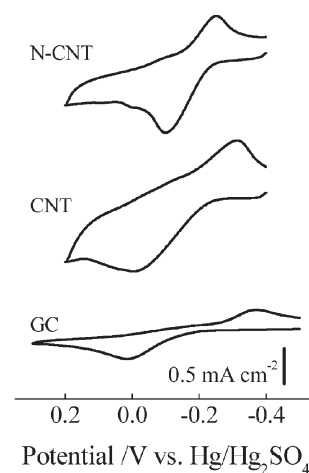


Fig. 6 Cyclic voltammograms of 1.0 mM DOPAC in 0.1 M acetate buffer (pH = 5.8) at N-CNT (top), non-doped CNT (middle), and GC (bottom) electrodes. Scan rate = 0.1 V s^{-1} .

at neutral pH ($\text{p}K_{\text{A}} \sim 4$) should show reduced peak splitting due to promotion of favorable electrostatic interactions. Voltammograms for the DOPAC/DOPAC orthoquinone couple are shown in Fig. 6. The N-CNTs demonstrate good reversibility ($\Delta E_{\text{p}} = 150 \text{ mV}$) for DOPAC oxidation, improved relative to the reversibility of dopamine and norepinephrine voltammetry in Figs. 3 and 5. In contrast, both the non-doped CNTs and GC electrodes exhibit much poorer DOPAC oxidation reversibility, suggesting *ca.* two orders of magnitude smaller values of k_{obs}° than the N-CNTs. We attribute the increased k_{obs}° at N-CNTs to the favorable attraction of the positive surface charge of the N-CNTs and the negative charge of DOPAC at pH 5.8. It may also be important that the increased surface charge and basicity of the N-CNTs further facilitates catecholamine and catechol oxidation, as N-CNTs have shown an increased sensitivity to the acid/base character of the supporting electrolyte for oxygen reduction relative to other carbon materials.⁵⁶ While it is premature in this report to identify the specific mechanistic step(s) that affect the voltammetry at N-CNTs, it is clear that in both cases of either cationic (dopamine and norepinephrine) or anionic (DOPAC) redox probes, N-CNTs demonstrate electrochemical responses that are unlike other clean graphitic electrode materials (non-doped CNTs and GC). To our knowledge, this is the first report of “as prepared” carbon electrodes that show improved sensitivity and selectivity towards electrooxidation of anionic catechols without extensive surface pretreatment or activation. The data presented herein demonstrate the unique surface character and basicity of N-CNTs that may be adventitious as inherently selective biochemical sensor materials.

Conclusions

As prepared non-doped and nitrogen-doped carbon nanotube electrodes demonstrate good electrochemical oxidative behavior for dopamine and norepinephrine. Semiintegral analysis of the oxidative portions of voltammograms for dopamine and norepinephrine highlight the activity of both non-doped and N-CNTs for catecholamine adsorption, with N-CNTs demonstrating approximately two-fold greater surface coverage in agreement with the 2.4 times greater edge plane content

measured with Raman spectroscopy. Larger peak splitting in catecholamine voltammetry and smaller peak splitting in DOPAC voltammetry at N-CNTs than at non-doped carbon electrodes suggest a possible electrostatic bias against facile oxidation of cationic catecholamines, but a preference for oxidation of anionic catechols like DOPAC.

Acknowledgements

Financial support of this work was provided in part by the R. A. Welch Foundation (Grant F-1529), the NSF (grant CHE-0134884) and the Strategic Partnership for Research in Nanotechnology (SPRING). We also acknowledge the NSF MRI program (grant CHE-0216443) for acquisition of the Raman microprobe. S. Maldonado acknowledges the Harrington Foundation and the NSF for fellowship support.

References

- 1 D. Adams, D. F. Williams and J. Hill, *J. Biomed. Mater. Res.*, 1978, **12**, 35.
- 2 F. Gonon, R. Cespuglio, J. L. Ponchon, M. Buda, M. Jouvett, R. N. Adams and J. F. Pujol, *C. R. Seances Acad. Sci., Ser. D*, 1978, **286**, 1203.
- 3 J. Millar, J. Stamford and R. M. Wightman, *J. Physiol. (London)*, 1984, **357**, P14.
- 4 M. A. Dayton, G. E. Geier and R. M. Wightman, *Life Sci.*, 1979, **24**, 917.
- 5 K. Kinoshita, *Carbon: Electrochemical and Physicochemical Properties*, John Wiley and Sons, Inc., New York, 1988, pp. 443–453.
- 6 F. G. Gonon, C. M. Fombarlet, M. J. Buda and J. F. Pujol, *Anal. Chem.*, 1981, **53**, 1386.
- 7 R. A. Saraceno and A. G. Ewing, *Anal. Chem.*, 1988, **60**, 2016.
- 8 S. H. DuVall and R. L. McCreery, *Anal. Chem.*, 1999, **71**, 4594.
- 9 C. D. Allred and R. L. McCreery, *Anal. Chem.*, 1992, **64**, 444.
- 10 L. Falat and H. Y. Cheng, *Anal. Chem.*, 1982, **54**, 2108.
- 11 S. Sujaritvanichpong, K. Aoki, K. Tokuda and H. Matsuda, *J. Electroanal. Chem.*, 1986, **198**, 195.
- 12 R. M. Wightman, E. C. Paik, S. Borman and M. A. Dayton, *Anal. Chem.*, 1978, **50**, 1410.
- 13 R. J. Bowling, R. T. Packard and R. L. McCreery, *J. Am. Chem. Soc.*, 1989, **111**, 1217.
- 14 G. M. Swain and T. Kuwana, *Anal. Chem.*, 1992, **64**, 565.
- 15 M. Poon, R. L. McCreery and R. Engstrom, *Anal. Chem.*, 1988, **60**, 1725.
- 16 R. J. Rice, N. M. Pontikos and R. L. McCreery, *J. Am. Chem. Soc.*, 1990, **112**, 4617.
- 17 B. Kazee, D. E. Weisshaar and T. Kuwana, *J. Am. Chem. Soc.*, 1985, **57**, 2736.
- 18 E. Popa, H. Notsu, T. Miwa, D. A. Tryk and A. Fujishima, *Electrochem. Solid-State Lett.*, 1999, **2**, 49.
- 19 M. Inagaki and L. R. Radovic, *Carbon*, 2002, **40**, 2279.
- 20 S. Subramoney, *Adv. Mater. (Weinheim, Ger.)*, 1998, **10**, 1157.
- 21 T. Belz, E. Sanchez, J. Yang, R. Schoonmaker, H. Sauer, J. Find, D. Herein, G. Wortmann and R. Schlogl, *Proc.-Electrochem. Soc.*, 1998, **98-8**, 169.
- 22 E. Sanchez, Y. Yang, J. Find, T. Braun, R. Schoonmaker, T. Belz, H. Sauer, O. Spillecke, Y. Uchida and R. Schlogl, *Stud. Surf. Sci. Catal.*, 1999, **121**, 317.
- 23 R. C. Mani, M. K. Sunkara, R. P. Baldwin, J. Gullapalli, J. A. Chaney, G. Bhimarasetti, J. M. Cowley, A. M. Rao and R. Rao, *J. Electrochem. Soc.*, 2005, **152**, E154.
- 24 B. S. Sherigara, W. Kutner and F. D'Souza, *Electroanalysis*, 2003, **15**, 753.
- 25 W. C. Poh, K. P. Loh, W. D. Zhang, S. Triparthy, J.-S. Ye and F.-S. Sheu, *Langmuir*, 2004, **20**, 5484.
- 26 P. J. Britto, K. S. V. Santhanam and P. M. Ajayan, *Bioelectrochem. Bioenerg.*, 1996, **41**, 121.
- 27 Z. H. Wang, J. Liu, Q. L. Liang, Y. M. Wang and G. Luo, *Analyst*, 2002, **127**, 653.
- 28 W. Zhang, Y. F. Xie, S. Y. Ai, F. L. Wan, J. Wang, L. T. Jin and J. Y. Jin, *J. Chromatogr., B*, 2003, **791**, 217.
- 29 C. E. Banks, R. R. Moore, T. J. Davies and R. G. Compton, *Chem. Commun.*, 2004, 16, 1804.
- 30 C. E. Banks, T. J. Davies, G. G. Wildgoose and R. G. Compton, *Chem. Commun.*, 2005, 7, 829.
- 31 R. R. Moore, C. E. Banks and R. G. Compton, *Anal. Chem.*, 2004, **76**, 2677.
- 32 S. Maldonado and K. J. Stevenson, *J. Phys. Chem. B*, 2004, **108**, 11375.
- 33 S. Maldonado and K. J. Stevenson, *J. Phys. Chem. B*, 2005, **109**, 4707.
- 34 M. Endo, *Chem.-Tech.*, 1988, **18**, 568.
- 35 J. A. Menendez, J. Phillips, B. Xia and L. R. Radovic, *Langmuir*, 1996, **12**, 4404.
- 36 L. C. A. Oliveira, C. N. Silva, M. I. Yoshida and R. M. Lago, *Carbon*, 2004, **42**, 11, 2279.
- 37 P. Chen, M. A. Fryling and R. L. McCreery, *Anal. Chem.*, 1995, **67**, 3115.
- 38 A. J. Bard and L. R. Faulkner, *Electrochemical Methods: Fundamentals and Applications*, John Wiley and Sons, Inc., New York, 2001, pp. 242–243.
- 39 Y. Xie and P. M. A. Sherwood, *Chem. Mater.*, 1990, **2**, 293.
- 40 G. N. Kamau, W. S. Willis and J. F. Rusling, *Anal. Chem.*, 1985, **57**, 545.
- 41 G. E. Cabaniss, A. A. Diamantis, W. R. Murphy, R. W. Linton and T. J. Meyer, *J. Am. Chem. Soc.*, 1985, **107**, 1845.
- 42 H. Estrade-Szwarckopf, *Carbon*, 2004, **42**, 1713.
- 43 S. Biniak, M. Walczyk and G. S. Szymanski, *Fuel Process. Technol.*, 2002, **79**, 251.
- 44 W. F. Chen, F. S. Cannon and J. R. Rangel-Mendez, *Carbon*, 2005, **43**, 581.
- 45 A. Cuesta, P. Dhamelincourt, J. Laureyns, A. Martinezalonso and J. M. D. Tascon, *Carbon*, 1994, **32**, 1523.
- 46 Y. Wang, D. C. Alsmeyer and R. L. McCreery, *Chem. Mater.*, 1990, **2**, 557.
- 47 F. Tuinstra and J. L. Koenig, *J. Chem. Phys.*, 1970, **53**, 1126.
- 48 P. Ramesh, G. S. Suresh and S. Sampath, *J. Electroanal. Chem.*, 2004, **561**, 173.
- 49 R. L. McCreery, in *Carbon Electrodes: Structural Effects on Electron Transfer Kinetics*, ed. A. J. Bard, Dekker, New York, 1991.
- 50 I. Morcos and E. Yeager, *Electrochim. Acta*, 1970, **15**, 953.
- 51 R. Bowling and R. L. McCreery, *Anal. Chem.*, 1988, **60**, 605.
- 52 S. H. DuVall and R. L. McCreery, *J. Am. Chem. Soc.*, 2000, **122**, 6759.
- 53 S. Ranganathan, T. C. Kuo and R. L. McCreery, *Anal. Chem.*, 1999, **71**, 3574.
- 54 M. D. Hawley, S. V. Tatawawadi, S. Piekarski and R. N. Adams, *J. Am. Chem. Soc.*, 1966, **89**, 447.
- 55 M. R. Deakin, P. M. Kovach, K. J. Stutts and R. M. Wightman, *Anal. Chem.*, 1986, **58**, 1474.
- 56 S. Maldonado and K. J. Stevenson, 2005, unpublished results.